Can COBE see the shape of the universe?

Neil J. Cornish
Relativity Group, DAMTP, Cambridge University, Silver Street, Cambridge CB3 9EW, United Kingdom

David Spergel
Department of Astrophysical Sciences, Princeton University, Princeton, New Jersey 08544

Glenn Starkman
Department of Physics, Case Western Reserve University, Cleveland, Ohio 44106-7079
(Received 26 August 1997; revised manuscript received 16 January 1998; published 30 April 1998)

In recent years, the large angle COBE-DMR data have been used to place constraints on the size and shape of certain topologically compact models of the universe. Here we show that this approach does not work for generic compact models. In particular, we show that compact hyperbolic models do not suffer the same loss of large angle power seen in flat or spherical models. This follows from applying a topological theorem to show that generic hyperbolic three manifolds support long wavelength fluctuations, and by taking into account the dominant role played by the integrated Sachs-Wolfe effect in a hyperbolic universe. [S0556-2821(98)05310-7]

PACS number(s): 98.70.Vc, 98.80.Cq, 98.80.Hw

In 1966, Kac [1] posed the question ''Can one hear the shape of a drum?'' In recent years a similar question has been asked in cosmology: ''Can one see the shape of the universe?'' [2]. More formally, the question can be phrased: can we discern the global topology of the universe by studying fluctuations in the cosmic microwave background (CMB) radiation?

With the launch of new satellites next century, and with a careful search for matched microwave temperatures around pairs of circles on the last scattering surface (''topological lensing'') [3,4], we should be able to answer this question in the affirmative. In the interim, we can ask how much can be done with the 4-year Cosmic Background Explorer (COBE) Differential Microwave Radiometer (DMR) data [5]. Poor angular resolution and low signal to noise make the COBE data unsuitable for direct lensing studies, but several groups [6–10] have used the data to put constraints on a variety of toroidal models. Here we consider how their results might be generalized to encompass a wider class of small universe models.[1] In particular we will be interested in hyperbolic models since observations suggest we live in a negatively curved universe. Moreover, the topology scale and the curvature scale are intimately related in hyperbolic models, whereas in a flat universe there is no scale at which one would expect to observe the topology. By applying a number of results pertaining to the topology of three manifolds, and by taking into account the integrated Sachs-Wolfe effect, we argue that *generic* small universe models cannot be constrained by COBE data. Naturally, some specific models can be constrained by COBE data, but we argue these are the exception rather than the rule.

Small universes enjoy the same local geometry and dynamics as the usual simply connected Friedmann-Robertson-Walker (FRW) models,[2] but display different global characteristics. In particular, small universes have a discrete spectrum of eigenmodes and are globally anisotropic and inhomogeneous. In models with locally spherical or Euclidean geometry the eigenvalue spectrum is raised above that of the simply connected models and there is a corresponding long wavelength cut-off. For example, the eigenvalues of the Laplacian on flat Euclidean space take all values in the range $k \in [0,\infty)$, corresponding to wavelengths $\lambda = 2\pi/k \in (\infty,0]$. However, if we compactify this space by making the identifications $(x,y,z) = (x+n_x L, y+n_y L, z+n_z L)$ where the n_i are integers, the eigenvalue spectrum becomes discrete, $k_n = 2\pi/L(n_x^2+n_y^2+n_z^2)^{1/2}$, and the bottom of the spectrum is raised from $k=0$ to $k=2\pi/L$. There is then a corresponding long wavelength cut-off $\lambda_{\max} = L$.

Assuming that temperature fluctuations in the CMB are caused by density fluctuations on the last scattering surface, this long wavelength cut-off is translated into a suppression of large angle power [6,7]. The cut-off in long wavelength power that occurs in Euclidean space was first used by Sokolov [6] to show that a flat universe with toroidal spatial sections could not be much smaller than the horizon size. He argued that the topology scale had to be large enough to allow the wavelengths needed to produce the quadrapole anisotropy measured by COBE. A number of groups [7–9] have since improved on Sokolov's bound and extended his analysis to include other flat topologies. Recently, Levin *et al.* [10] have generalized these bounds to include a noncompact, infinite volume hyperbolic topology describing a toroidal horn.

There has been a tendency to draw general conclusions from these few examples. Indeed, the small universe idea

[1] A small universe is defined to be one that is multiply connected on scales smaller than the particle horizon.

[2] By simply connected we mean the fundamental group $\pi_1(\Sigma)$ is trivial. Since $\pi_1(S^3) = \pi_1(E^3) = \pi_1(H^3) = \mathbf{I}$, the usual FRW models are all simply connected. A multiply connected model has a nontrivial fundamental group.

was declared dead in Ref. [8]. While it is fair to say that positively curved small universes, and the simplest toroidal flat universes with topology scale much less than the horizon scale are effectively ruled out [9], we show that the same cannot be said about negatively curved models. Lessons learned in flat space do not always apply in hyperbolic space. For example, the eigenvalue spectrum is typically *lowered*, rather than raised by making hyperbolic space compact, i.e. k^2 can be less than zero. Consequently, there need not be a long wavelength cut-off. Even if there were, and even assuming a simple initial power spectrum at large wavelengths, the existence of large angle power as measured by COBE-DMR still could not directly be used to constrain compact hyperbolic models since the large angle power in a negatively curved universe does not come from the last scattering surface. The bulk of the large angle power is due to the decay of curvature perturbations along the line of sight [11–13]. If the universe is hyperbolic, COBE has been detecting fluctuations produced at moderate redshifts $z<5$, rather than $z\sim 1200$. Consequently, the large angle power is produced by fluctuations occurring on small comoving length scales that only appear large due to their relatively close proximity.

In Sec. I we briefly discuss constraints on small universe models based on searches for ghost images. In Sec. II we emphasize the importance of the ISW effect for calculating CMB fluctuations on large angular scales. In Sec. III we describe the eigenmodes of infinite hyperbolic space. Section IV contains an introduction to compact hyperbolic space and its underlying mathematical structure. In Sec. V we obtain lower limits on the wavelength of the longest wavelength mode, showing that modes with wavelengths longer than the curvature scale usually exist, though in what multiplicity we cannot say. In Sec. VI we digress to consider a particular class of topologies closely related to the horn topology studied by Levin *et al.* [10]. In Sec. VII we speculate about the form of the primordial power spectrum in compact models, and describe how the mixing property of compact hyperbolic space tends to spread power across a wide range of angular scales. Our conclusions can be found in Sec. VIII. A glossary of mathematical terms is included in the Appendix. References to words appearing in the glossary are indicated in the text by roman superscripts, e.g. Betti number.[a]

Throughout the paper we will be assuming that a cosmological constant does not provide a significant contribution to the density of the universe.

I. GHOST HUNTING

The most obvious observational signature of a multiply connected universe would be repeated or ''ghost'' images of familiar objects such as galaxies or rich clusters [14]. However, searches for ghost images are hampered by evolution of the objects; our ability to recognize objects when viewed from different directions; and the difficulty in determining the distances to objects.

Despite these problems, the consensus seems to be that there is no evidence for ghost images out to redshifts of $z\sim 0.4$—the current depth of wide-field redshift surveys. It is interesting to note that this lack of ghost images is exactly what one expects for typical small compact hyperbolic models. According to Thurston [15], the expectation value for the length of the shortest closed geodesics in a typical small hyperbolic universe is roughly $(0.5\rightarrow 1.0)R_0$, where $R_0 = H_0^{-1}/\sqrt{1-\Omega_0}$ is the comoving curvature radius. Here H_0 is the Hubble constant and Ω_0 is the matter density in units of the critical density. The first copies of the Milky Way galaxy or Coma cluster would not be seen before a conformal lookback time of $\eta\simeq 0.5\rightarrow 1.0$. Converting this to redshift space via the relation

$$1+z=\frac{2(\Omega_0^{-1}-1)}{\cosh(\eta_0-\eta)-1}, \tag{1.1}$$

where $\eta_0=\operatorname{arccosh}(2/\Omega_0-1)$ is the present conformal time, we find that the first ghost images will be at a redshift of $z\simeq 0.9\rightarrow 2.9$ in a universe with $\Omega_0=0.3$. If the universe has Ω_0 closer to unity, the first ghost images will be even more distant.

These numbers suggest that direct searches for ghost images of astrophysical objects will be unable to tell if we live in a compact hyperbolic universe. A more promising approach is to look for topological lensing of the last scattering surface by studying fluctuations in the cosmic microwave background radiation [3,4].

II. MICROWAVE BACKGROUND FLUCTUATIONS

Conventional lore holds that the finite size of a small universe will lead to a long wavelength cutoff in the spectrum of primordial fluctuations. In the sections to follow, we show that this is not guaranteed in a hyperbolic universe. In this section we point out that even if there were such a cut-off, it would be masked by the integrated Sachs-Wolfe (ISW) effect on the angular scales probed by COBE.

In adiabatic models (e.g. inflation) the primordial fluctuation spectrum determines the power spectrum on the last scattering surface. However, the fluctuations measured by COBE do not necessarily originate on the last scattering surface. In a negatively curved universe, power on angular scales larger than the curvature scale is produced at relatively low redshifts by fluctuations occurring on scales considerably smaller than the curvature scale. This severely limits COBE's ability to probe the large scale topology of the universe.

In a hyperbolic universe, there are two terms that produce the microwave background fluctuations on large angular scales:

$$\frac{\Delta T(\theta,\phi)}{T}=\frac{\Phi(\mathbf{x}_{sls},\eta_{sls})}{3}+2\int_{\eta_{sls}}^{\eta_0}\dot{\Phi}(\mathbf{x},\eta)\,d\eta, \tag{2.1}$$

where η_{sls} is the conformal time at the surface of last scatter and η_0 is the present conformal time. The first term is due to variations in the gravitational potential and photon density at the surface of last scatter. The latter term, which is zero to linear order in a matter dominated *flat* universe, is due to the decay of potential fluctuations at late times, $(1+z)<\Omega_0^{-1}$. In a universe with $\Omega_0=0.3$, the latter term, the so-called integrated Sachs-Wolfe effect, is the *dominant* source of microwave background fluctuations on large angular scales [13]. The late-time ISW effect dominates multipole moments be-

low $\ell_{\rm curv}=2\sqrt{1-\Omega_0}/\Omega_0$. Neglecting this contribution will lead to a severe underestimate of the large angle power.

Because of the late-time ISW effects, we expect significant large angular scale fluctuations even if Ω_0 is as small as 0.1. Kamionkowski and Spergel [13] calculated the CMB fluctuations in hyperbolic models with trivial topology and a variety of primordial power spectra. Below the curvature scale the standard scale-invariant Harrison-Zeldovich spectrum was used. This is probably reasonable at sufficiently small scales for models with non-trivial topology, including compact models, as small scale perturbations will be less sensitive to global properties such as the curvature and topology. Beyond the curvature scale, both the unknown form of the eigenmodes and the expected effects of transients in the inflationary dynamics make the situation much less clear. For the latter reason, Kamionkowski and Spergel considered a range of power spectra. Of the models they considered, the ''volume power law model'' has the least long wavelength power. In this model, fluctuations on scales larger than the curvature scale are exponentially suppressed. Consequently, there is essentially no contribution to $\Delta T/T$ from the last scattering surface in the volume power law model. Nevertheless, the second term in Eq. (2.1) produced sufficient power to fit the fluctuations observed by COBE-DMR (see figures 6 and 9 in [13]).

The above result is not difficult to understand. As mentioned earlier, the large angle power in a sub-critical universe is produced by fluctuations occurring on small comoving length scales that only appear large due to their relatively close proximity. To make this concrete, we can consider the contribution $\alpha_\ell(k)$ to a given multipole, ℓ, from modes with wave number k [12]:

$$\alpha_\ell(k)=\Phi_k(\eta_0)\widetilde{\alpha}_\ell(k) \tag{2.2}$$

where

$$\widetilde{\alpha}_\ell(k)=\left[\frac{1}{3}F(\eta_{\rm sls})X_k^\ell(\eta_0-\eta_{sls}) + 2\int_{\eta_{sls}}^{\eta_0}\frac{dF}{d\eta}(\widetilde{\eta})X_k^\ell(\eta_0-\widetilde{\eta})d\widetilde{\eta}\right]. \tag{2.3}$$

Here X_k^ℓ are the radial eigenfunctions of the Laplacian on H^3 (see next section), and $\Phi_k(\eta)$ describes the curvature perturbation on scales $2\pi/k$ at conformal time η. These are related to the curvature perturbations today by $\Phi_k(\eta)=\Phi_k(\eta_0)F(\eta)/F(\eta_0)$ where [16]

$$F(\eta)=5\frac{\sinh^2(\eta)-3\eta\sinh\eta+4\cosh\eta-4}{(\cosh\eta-1)^3}. \tag{2.4}$$

In a flat universe $dF/d\eta=0$ to leading order, and only the first term contributes. Moreover, it is easy to show that $\widetilde{\alpha}_\ell(k)$ is strongly peaked at $k_{sls}\sim\ell+1$ in a flat universe if we chose our unit of length to be the radius of the surface of last scatter. The same is true in an open universe for multipoles with $\ell\gg\ell_{\rm curv}$, but for low multipoles the second term in Eq. (2.3) dominates. For example, Fig. 1 shows which modes k contribute most to the quadrapole integrand,

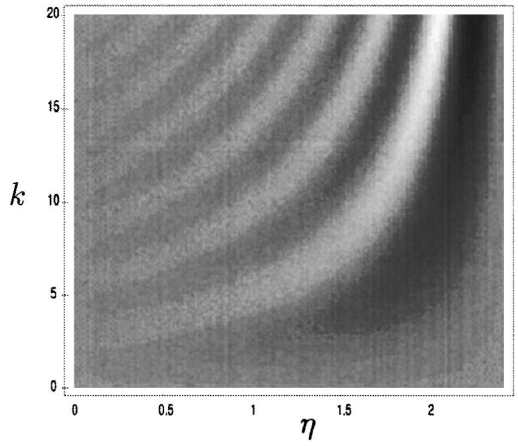

FIG. 1. A density plot showing the quadrapole integrand, $F'(\eta)X_k^2(\eta_0-\eta)$, as a function of wave number k and time since last scatter η. The regions of highest contrast are where the dominant contribution occurs.

$F'(\eta)X_k^2(\eta_0-\eta)$, in a universe with $\Omega_0=0.3$. Notice that the dominant contribution comes from late times, $\eta>1.5$, $z<2$ and large wave number.

We highlight the wave number dependence in Fig. 2 by plotting $|\widetilde{\alpha}_2(k)|$ and $|\alpha_2(k)|$. The latter is shown for a volume power law scaling with spectral index $n=1$. We see that the dominant contribution to the quadrapole comes from modes with wave numbers $k\sim3\rightarrow10$ in curvature units or $k_{sls}\sim7\rightarrow24$ in units of the radius of the surface of last scatter. This should be contrasted with the flat space case where modes with $k_{sls}\sim2\rightarrow4$ provide the dominate contribution to the quadrapole.

The important lesson in all this for compact hyperbolic models is that the form of the power spectrum at very small wave number (long wavelength) is largely irrelevant. It is power on scales smaller than the curvature scale that contributes most to the low multipoles. Since the topology scale is typically comparable to or larger than the curvature scale, the ISW effect should ensure there is no significant suppression of the large angle temperature fluctuations in generic compact models.

In contrast to the amplitude fluctuations, microwave background polarization fluctuations exclusively probe the surface of last scatter. These fluctuations arise due to electron

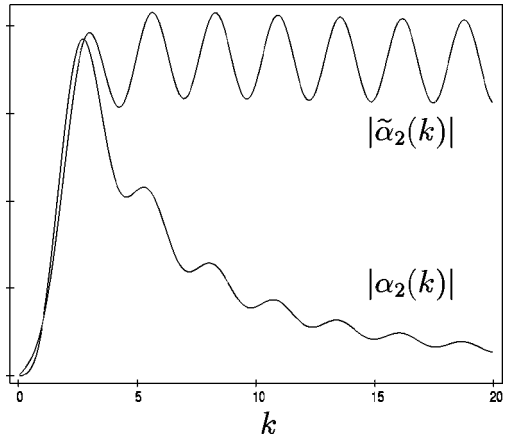

FIG. 2. The functions $|\widetilde{\alpha}_2(k)|$ and $|\alpha_2(k)|$ in a universe with $\Omega_0=0.3$. The scaling is arbitrary.

scattering and depend on gradients in the velocity field [17,18]

$$(Q+iU)(\hat{\mathbf{n}})=0.17\Delta\tau_*\mathbf{m}^i\mathbf{m}^j\partial_i v_j|_{\tau_*} \tag{2.5}$$

where $\Delta\tau_*$ is the width of the last scattering surface and is giving a measure of the distance photons can travel between their last two scatterings. Here, Q and U are the Stokes parameters, $\mathbf{n}$ is the direction of photon propagation, and $\mathbf{m}=\widehat{\mathbf{e}_1}+i\widehat{\mathbf{e}_2}$, where $\widehat{\mathbf{e}_1}$ and $\widehat{\mathbf{e}_2}$ form a basis orthogonal to $\mathbf{n}$. Note that polarization fluctuations are produced only due to scattering and are not sensitive to the ISW effects. Thus, polarization fluctuations are our best chance to directly probe supercurvature modes.

III. VIBRATIONS IN A HYPERBOLIC CAVITY

When attempting to calculate perturbation spectra in compact hyperbolic space one is immediately confronted by the highly non-trivial task of finding the eigenmodes. In principle the eigenmodes of a compact space can be obtained from the eigenmodes of the simply connected covering space using the method of images [19]. In practice the sums involved are highly divergent and can only be tamed by sophisticated resummation methods [20,21]. Before confronting this challenging problem we need to know the eigenmodes of the covering space. The covering space has the metric

$$\begin{aligned} ds^2&=dt^2-R^2(t)d\sigma^2,\\ &=R^2(\eta)(d\eta^2-d\sigma^2), \end{aligned} \tag{3.1}$$

where the $d\sigma^2$ is the metric on hyperbolic three-space,

$$d\sigma^2=d\chi^2+\sinh^2\chi(d\theta^2+\sin^2\theta d\phi^2). \tag{3.2}$$

The Ricci curvature of this metric is -1, corresponding to a curvature scale of unity. Perturbations in such a spacetime can be expanded in terms of spherically symmetric solutions of the Helmholtz equation $(\Delta+q^2)Q=0$, where the Δ is the Laplace operator on H^3,

$$\begin{aligned} \Delta Q=\frac{1}{\sinh^2\chi}\Bigg[&\frac{\partial}{\partial\chi}\left(\sinh^2\chi\frac{\partial Q}{\partial\chi}\right)+\frac{1}{\sin^2\theta}\frac{\partial}{\partial\theta}\left(\sin\theta\frac{\partial Q}{\partial\theta}\right)\\ &+\frac{1}{\sin^2\theta}\frac{\partial^2 Q}{\partial\theta^2}\Bigg]. \end{aligned} \tag{3.3}$$

The eigenfunctions are given by [22]

$$Q^{q\ell m}(\chi,\theta,\phi)=X_q^\ell(\chi)Y_\ell^m(\theta,\phi), \tag{3.4}$$

where the Y_ℓ^m's are spherical harmonics and the radial eigenfunctions are given by

$$X_q^\ell(\chi)=\frac{(-1)^{\ell+1}\sinh^\ell\chi}{\left[\prod_{n=0}^{l}(n^2+k^2)\right]^{1/2}}\frac{d^{\ell+1}\cos(k\chi)}{d(\cosh\chi)^{\ell+1}}. \tag{3.5}$$

The wave number, $k=2\pi/\lambda$, is related to the eigenvalues of the Laplacian by

$$k^2=q^2-1. \tag{3.6}$$

In the literature there is considerable confusion surrounding this shift between eigenvalue and wave number in hyperbolic space. Some authors claim that q is the wave number, but this is not true. Indeed, it is simple to prove that for $\chi>2\pi/k$, the radial eigenfunctions take the form

$$X_q^\ell(\chi)\sim\frac{\cos(k\chi+\phi_{k\ell})}{\sinh\chi}, \tag{3.7}$$

where $\phi_{k\ell}$ is a k,ℓ dependent phase. The $1/\sinh\chi$ factor follows from flux conservation in a space where the surface area of a ball grows as $4\pi\sinh^2\chi$. Clearly, k is the wave number and $\lambda=2\pi/k$ is the wavelength. We will refrain from calling modes with $\lambda>1$ ''supercurvature'' to avoid confusion with other papers in the literature where ''supercurvature'' is used to describe modes with $q^2<1$. Perhaps the confusion surrounding wave numbers in open models comes from considering the wave equation for massless scalar fields:

$$\left(\frac{\partial^2}{\partial\eta^2}-\Delta\right)\Psi(\eta,\mathbf{x})=0. \tag{3.8}$$

For eigenmodes $\Psi(\eta,\mathbf{x})$ with eigenvalue q and angular frequency ω_q we have

$$\omega_q^2=q^2=k^2+1=\frac{(2\pi)^2}{\lambda^2}+1. \tag{3.9}$$

Notice that the usual relationship between frequency and wavelength is offset by one unit. If we were to neglect this offset and assert that $\omega=2\pi/\lambda$, then we would erroneously conclude that q was the wave number.

In compact hyperbolic space the eigenmodes will be discrete and the spectrum can be *lowered* below $k^2=0$. Modes with $k^2<0$ are not square integrable in infinite hyperbolic space as they grow exponentially with χ. However, these modes are square integrable in compact hyperbolic space and are thus quite acceptable.

The physical and comoving counterparts to the wave number k and wavelength λ are scaled such that

$$\begin{aligned} k_{\rm phys}&=\frac{k}{R(t)}, \quad k_{\rm cmvg}=\frac{k}{R_0}=kH_0\sqrt{1-\Omega_0},\\ \lambda_{\rm phys}&=R(t)\lambda, \quad \lambda_{\rm cmvg}=R_0\lambda=\frac{\lambda}{H_0\sqrt{1-\Omega_0}}. \end{aligned} \tag{3.10}$$

Fluctuations in the temperature of the cosmic microwave background are due to variations in the gauge invariant gravitational potential $\Phi(\mathbf{x},\eta)$. The connection between eigenvalue spectra and observed fluctuations in the CMB follows from the relation

$$\Phi(\mathbf{x})=\sum_{q,\ell,m}c_{q\ell m}Q^{q\ell m}(\mathbf{x}). \tag{3.11}$$

The expansion coefficients $c_{q\ell m}$ are fixed by the primordial power spectrum. Moreover, any physical mechanism for generating that primordial power will be influenced by the shape of the eigenmodes and the eigenspectrum, for no matter how skilled the drummer, a snare drum will not sound like a timpani.

IV. COMPACT HYPERBOLIC SPACE

A compact hyperbolic universe has spatial sections of the form $\Sigma = H^3/\Gamma$, where the fundamental group, Γ, is a discrete subgroup of $SO(3,1) \cong PSL(2,C)$ acting freely (i.e. without fixed points) and discontinuously (since it is discrete). According to Poincare's fundamental polyhedron theorem [23], Σ can be obtained by gluing together the faces of a polytope in hyperbolic space. The polytope is otherwise referred to as the manifold's fundamental cell or Dirichlet domain.[3]

Any function defined on the compact space $\Sigma = H^3/\Gamma$ must be invariant under the action of the fundamental group $\Gamma \subset SO(3,1)$. The simplest way to enforce this condition employs the method of images:

$$Q_\Gamma(\mathbf{x}) = \sum_{g \in \Gamma} Q(g\mathbf{x}). \tag{4.1}$$

The same method can be used to generate any n-point function in the compact space via a sum over translated copies of the corresponding function in the covering space. In a recent paper, Bond *et al.* [24] applied the method of images to the two-point correlation function in several compact hyperbolic universes. They concluded that several of the smaller volume hyperbolic models were incompatible with the COBE data. However, in this preliminary study they did not include the ISW effect, nor did they demonstrate that their results are independent of the infrared regularization scheme they used. They [25] recently reported a new analysis that includes the ISW effect and appears to be consistent with our conclusion that COBE is compatible with compact manifolds.

Hyperbolic 3-space can be viewed as the unit hyperboloid (mass-shell)

$$-x_0^2 + x_1^2 + x_2^2 + x_3^2 = -1, \tag{4.2}$$

embedded in four-dimensional Minkowski space. We can relate this representation to the induced metric on H^3, (3.2), by the coordinate identifications

$$x_0 = \cosh\chi, \quad x_1 = \sinh\chi\cos\theta, \quad x_2 = \sinh\chi\sin\theta\cos\phi,$$

$$x_3 = \sinh\chi\sin\theta\sin\phi. \tag{4.3}$$

From this perspective it is easy to understand why the isometries of H^3 are described by the orientation preserving homogeneous Lorentz group in four-dimensions, $SO(3,1)$.

[3]A simple analogue in two dimensions is the torus, E^2/Γ, where E^2 is the plane and Γ is the group generated by a translations by L_x in the x direction, and L_y in the y direction. The fundamental cell for this torus is a rectangle with opposite faces identified.

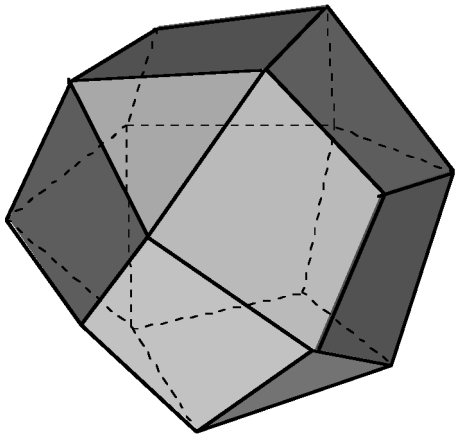

FIG. 3. The fundamental cell for Thurston's manifold.

Given a set of generators $\{a_1,..,a_j\}$, any element of the fundamental group Γ can be written as

$$g = \prod_i a_{m_i}^{j_i} \quad (i, j_i, m_i \in \mathbf{Z}), \tag{4.4}$$

with possible repetitions of the generators. The group element g is called a word, and the length of the word is defined to be

$$l_g = \sum_i |j_i|. \tag{4.5}$$

Not all words generated according to Eq. (4.4) will be unique since the generators are typically subject to a set of relations, *e.g.* $a_1 a_2 a_1^{-2} a_2 = 1$. The number of distinct words with lengths less than or equal to l is denoted $\mathcal{N}(l)$. A theorem due to Milnor [26] tells us that $\mathcal{N}(l)$ grows exponentially with l if Γ is the fundamental group of a compact hyperbolic manifold. It is precisely this exponential growth that causes problems with the sum over images. The rate of growth is measured by the grammatical complexity or topological entropy of the fundamental group, $H_T = \lim_{l\to\infty} l^{-1} \log[\mathcal{N}(l)]$.

To illustrate the preceeding discussion we use SNAPPEA [27] to study Thurston's manifold [28], $\Sigma_{\rm Th}$ [m003(−2,3) in the SNAPPEA census]. The fundamental group, $\Gamma = \pi_1(\Sigma_{\rm Th})$, has the presentation[4]

$$\Gamma = \{a,b : a^2 b a^{-1} b^3 a^{-1} b, \quad ababa^{-1} b^{-1} a b^{-1} a^{-1} b\}. \tag{4.6}$$

The generators of the fundamental group describe identifications in the faces of the fundamental cell shown in Fig. 3. The fundamental cell is drawn using Klein's projective model for hyperbolic space. In this projection H^3 is mapped into an open ball in E^3. Under this mapping hyperbolic lines and planes are mapped into their Euclidean counterparts. This is why the totally geodesic faces of the fundamental cell appear as flat planes.

Thurston's manifold has volume 0.98137, symmetry group $G = \{u,v : u^2, v^2, uvuv\} = \mathbf{Z}_2 \oplus \mathbf{Z}_2$, first homology

[4]A presentation lists the group generators followed by any words which are equivalent to the identity.

group $\mathbf{Z}_5$ and Betti numbers[a] $b_0=b_3=1$, $b_1=b_2=0$. The symmetry group describes the symmetries of the manifold. The (first) homology group [29] is the Abelianized version of the fundamental group (4.6). When Abelianized, the relations obeyed by the fundamental group collapse down:

$$a^2ba^{-1}b^3a^{-1}b=1 \;\Rightarrow\; \tilde{b}^{\,5}=1$$

$$ababa^{-1}b^{-1}ab^{-1}a^{-1}b=1 \;\Rightarrow\; \tilde{a}=\tilde{b}^{-1}, \qquad (4.7)$$

leaving the homology group

$$H_1(\Sigma_{\mathrm{Th}})=\{\tilde{b}:\tilde{b}^{\,5}=1\}=\mathbf{Z}_5. \qquad (4.8)$$

Choosing a coordinate system centered at a maximum of the injectivity radius function,[b] the generators have the $SO(3,1)$ matrix representations

$$a=\begin{pmatrix} 1.4498 & -0.3191 & 0.8911 & -0.4538 \\ -0.5653 & -0.5653 & -0.8911 & 0.4538 \\ 0.8844 & -0.8844 & 0.8911 & -0.4538 \\ 0.0000 & 0.0000 & -0.4538 & -0.8911 \end{pmatrix}, \qquad (4.9)$$

and

$$b=\begin{pmatrix} 2.9351 & 2.4389 & -1.1390 & -0.6073 \\ 0.9195 & 0.4233 & -1.1390 & -0.6073 \\ 2.5987 & 2.5987 & -0.8587 & -0.5125 \\ 0.1255 & 0.1255 & -0.5125 & 0.8587 \end{pmatrix}. \qquad (4.10)$$

The image of any point $\mathbf{x}\in H^3$ can now be found by matrix multiplication. To give an example, the origin $\mathbf{x}=\mathbf{0}$ has $\chi=0$ and corresponds to the point $[1,0,0,0]$ when embedded in four-dimensional Minkowski space. Acting on this point by a takes it to the point $[1.450,-0.565,0.884,0]$. This point has $\chi=0.9161$, $\theta=2.1395$ and $\phi=0.0157$, and so lies a distance 0.9161 units away in 3-space.

Points lying on a symmetry axis of a group element will be translated the shortest distances. Conversely, the further a point lies from the symmetry axis of a group element, the further it is translated by that element. Since the fundamental group acts differently on different points, compact hyperbolic models are not homogeneous. Nor are they isotropic since there are preferred symmetry axes. Points on the symmetry axis of a group element can be located by finding the eigenvectors of the $SO(3,1)$ matrix describing the group element. The two real eigenvectors define points on the light cone enclosing the hyperboloid (4.2). The line passing through these two points defines the symmetry axis of the group element. The intersection of this line with the hyperboloid (4.2) defines the point in H^3 that is translated the shortest distance. For example, a has the two real eigenvectors

$$e_1=[-0.7491,0.3497,-0.6563,0.0896],$$

$$e_2=[0.7350,0.2687,-0.6460,0.2252], \qquad (4.11)$$

TABLE I. Minimal geodesics shorter than 2.

Length	Torsion	Word
0.57808244	2.13243064	ab
0.72156837	−1.15121299	b
0.889442997	2.94185905	a
0.998325189	−2.92101779	ab^{-1}
1.040315125	0.98237189	$aba^{-1}b$
1.793800843	−1.55687105	a^2b
1.822279900	−2.41353903	$ab^{-1}a^{-1}b$

and the line they define in Minkowski space intersects the hyperboloid at the point

$$v=[1.2428,0.2409,-0.6425,0.2716]. \qquad (4.12)$$

Acting on this point by a leads to the image point

$$v_a=[1.0292,-0.1431,0.19035,0.0496], \qquad (4.13)$$

a distance[5] 0.8894 units away in 3-space.

By acting on points lying on the symmetry axis of each group element it is possible to compile a list of the minimal geodesics. A typical isometry is a corkscrew-type motion, consisting of a translation of length L along a geodesic, combined with a simultaneous rotation through an angle ω about the same geodesic. The length and torsion can be found directly from the eigenvalues of the group element, and are conveniently listed by the SNAPPEA program [27]. Table I records both the length and the torsion of all geodesics with $L<2$.

Each word $g\in\Gamma$ does not necessarily produce a unique minimal geodesic. The minimal geodesic generated by ab^2 has the same length and torsion as that generated by b. The mapping between words and minimal geodesics is many to one. To make the mapping one to one, the words need to be grouped into conjugacy classes. Two words, g and g' belong to the same conjugacy class if and only if they are equal up to an isometry of[6] Γ:

$$g\sim g' \quad \text{iff} \quad g'=f^{-1}gf \quad (f\in\Gamma). \qquad (4.14)$$

A theorem by McKean [30] then states that there is a one-to-one correspondence between conjugacy classes of the fundamental group and the periodic geodesics. If we define Π_p to be the set of all geodesic loops at some point $p\in\Sigma$, endowed with the product $\gamma_a\bigcirc\gamma_b$ (first γ_b then γ_a) for all $\gamma_a,\gamma_b\in\Pi_p$, then Π_p is isomorphic to $\pi_1(\Sigma)=\Gamma$. This link between geodesic loops and the fundamental group can be used to re-express the sum over images (4.1) as a sum over periodic orbits. It is this principle that forms the basis of

[5]A simple way to work out the length of the shortest geodesic connecting two points is to first perform an $O(3,1)$ rotation of the coordinate system so that one of the points lies at the origin of H^3. The proper distance between the two points is then found by taking the arccosh of the other point's ''time'' coordinate, in accordance with Eq. (4.3).

[6]E.g., for Thurston's manifold we have $ab^2\sim bab\sim ababa^{-1}=b^{-1}aba^{-1}b\sim aba^{-1}\sim b$.

Gutzwiller's method [19] for determining the eigenmodes on compact hyperbolic space. Indeed, many of the techniques used to describe quantum chaos, including Gutzwiller's trace formula, have been developed using compact hyperbolic space as a laboratory [31]. The exponential growth in the number of words with symbolic lengths $l_g \leq l$ is echoed by the exponential growth in the number of closed geodesics with physical lengths $L_\gamma \leq L$:

$$N(L) \sim \frac{e^{hL}}{hL}, \tag{4.15}$$

where h is the Kolmogorov-Sinai (KS) entropy of the geodesic flow [31]. It is interesting to note that KS entropy scales as $h \propto V^{-1/3}$ while the topological entropy scales as $H_T \propto V$. This is because the KS entropy measures the rate of chaotic mixing, and smaller manifolds mix better, while the topological entropy measures the complexity of the fundamental group, and larger manifolds have more complicated topologies [32].

We can make some general observations about the existence of long wavelength modes on H^3/Γ based on SNAPPEA's listing of the short minimal geodesics. Typical closed geodesics, such as those listed in Table I for Thurston's manifold, involve a considerable torsion. A similar twisting occurs in 5 of the 6 compact, orientable flat three manifolds [33]. One example is $T^3_{1,\pi}$, where opposite faces of a cube are identified, with one pair of faces identified after a twist through π. If the cube has side length L, then the twisted minimal geodesic has length L and torsion π. As a consequence of this torsion, the lowest eigenmode along the twisted direction must wrap twice around $T^3_{1,\pi}$ before closing. The maximum allowed wavelength is thus $2L$, not L. We may anticipate a similar phenomenon occurring in hyperbolic space. The shortest geodesic listed in Table I has torsion $2.132431 \approx 2\pi/2.9465$. This geodesic approximately closes after 3 turns, but may never close exactly if it is an irrational multiple of 2π. Using this Bohr-Sommerfeld style reasoning, it appears likely that compact hyperbolic manifolds will admit very long wavelength modes.

V. LONG WAVELENGTH MODES

Here we study long wavelength modes in small hyperbolic universes. We do this without explicitly solving for the eigenmodes by exploiting the close connection between eigenvalue spectra and topology. We find a number of useful topological results pertaining to long wavelength modes.

For hyperbolic manifolds of dimension $d \geq 3$ there is a remarkable connection between geometry and topology. The rigidity theorem of Mostow-Prasad [34] proves that any connected and orientable manifold of dimension $d \geq 3$ supports at most one hyperbolic metric (up to diffeomorphisms). This means that geometrical quantities such as volume, injectivity radius,[c] diameter,[d] geodesic length spectra and eigenvalue spectra are all *topological invariants* for compact hyperbolic manifolds.

In this section we will put the topologists' interest in the eigenvalue spectra to good use. Without having to solve for the eigenmodes explicitly we can prove several results concerning the existence of long wavelength modes in compact hyperbolic spaces. In particular, we prove that generic compact hyperbolic spaces admit modes with wavelengths that exceed the curvature scale. In addition, we show that there exist finite volume, compact hyperbolic manifolds with an arbitrarily large number of modes with arbitrarily long wavelengths.

To relate these results to cosmology we need to recall the relationship between curvature, redshift, density and the radius of the surface of last scatter (SLS) in a hyperbolic universe. The curvature radius is fixed by the scale factor $R(t)$ since the metric (3.2) has unit curvature radius. The radius of the last scattering surface at redshift z is given by

$$R_{sls} = R \operatorname{arccosh}\left(1 + \frac{2(1-\Omega_0)}{\Omega_0(1+z)}\right) \equiv R\chi_{sls}. \tag{5.1}$$

The volume of space encompassed by the SLS is

$$V_{sls} = \pi R^3 (\sinh(2\chi_{sls}) - 2\chi_{sls}). \tag{5.2}$$

The radius of the last scattering surface today is approximately equal to the curvature radius if $\Omega_0 = 0.8$. If $\Omega_0 = 0.4$ we find $R_{sls} \approx 2R_0$; if $\Omega_0 = 0.1$ we find $R_{sls} \approx 3.6R_0$. The angle subtended by the curvature scale on the last scattering surface is approximately

$$\theta_{\rm curv} \approx 1.68 \frac{\Omega_0}{\sqrt{1-\Omega_0}}. \tag{5.3}$$

The above expression assumes that the universe has been matter dominated since decoupling. This will be true if matter-radiation equality was reached before decoupling so that

$$z_{\rm eq} = 24000\Omega_0 h^2 > z_{sls} \Rightarrow \Omega_0 h^2 > 0.052. \tag{5.4}$$

Assuming $h > 0.5$, Eq. (5.3) will be valid so long as $\Omega_0 > 0.2$. Since, roughly speaking, the $\ell^{\rm th}$ multipole moment measures power on angular scales[7] of π/ℓ, modes with $\lambda > 1$ probe angular scales $\ell < \ell_{\rm curv}$, where

$$\ell_{\rm curv} \approx \frac{2\sqrt{1-\Omega_0}}{\Omega_0}. \tag{5.5}$$

In a universe with $\Omega_0 = 0.5$, only the $\ell = 2$ quadrapole probes modes with $\lambda > 1$, while in a universe with $\Omega_0 = 0.3$ the range is increased to include all multipoles below $\ell = 6$. This tells us that perturbations with wavelengths larger than the curvature scale are responsible for the large angle power on the last scattering surface if $\Omega_0 < 0.5$.

Using Eq. (5.2) we can estimate the redshift when a fundamental cell first dropped within the last scattering surface from the relation

[7]The reasoning being that the $\ell^{\rm th}$ multipole has 2ℓ zeros in the range $\theta \in [-\pi, \pi]$, with approximately equal spacings of $\Delta\theta = \pi/\ell$.

$$1+z=\frac{2(\Omega_0^{-1}-1)}{\Omega_0(\cosh r_+-1)}, \tag{5.6}$$

where r_+ is the outradius[e] of the manifold. Taking Thurston's manifold [28] (see Fig. 3) with $\mathrm{Vol}(\Sigma_{\mathrm{Th}})=0.98137$ and $r_+=0.748537$ as a particular example, we find that the fundamental cell dropped inside the SLS no earlier than $z=9.2$ if $\Omega_0=0.4$. Today there would be approximately 86 copies of the fundamental cell within the SLS (this is the ratio of volume of the optically observable universe to the comoving volume of Thurston's manifold). Since the volume of a hyperbolic manifold is a measure of topological complexity, Thurston's manifold ranks as one of the simplest topologies the universe can have. The only known example that is simpler is the Weeks manifold with volume 0.9427 . . . . It is thought that the Weeks manifold is *the* smallest hyperbolic three manifold, though the most recent lower bound, $\mathrm{Vol}(\Sigma_{\mathrm{min}})>0.166$ [35] still leaves some room for smaller, simpler topologies.

Returning to our treatment of the eigenvalues, we introduce the ordering $0=q_0<q_1<q_2\ldots$, where the eigenvalues are counted with their multiplicities. The mathematical literature is littered with dozens of upper and lower bounds for the q_j's in terms of the volume, diameter or isoperimetric constant of a manifold. Unfortunately most of these bounds are not very sharp since the results apply to a great variety of manifolds. Sharper bounds can probably be found by restricting one's attention to three dimensional manifolds with constant negative curvature.

Most papers deal with the first eigenvalue, q_1, whereas we are most interested in eigenmodes with $q^2\in[1,1+\epsilon^2]$ where $\epsilon\ll 1$. Eigenmodes in this interval correspond to modes with wavelengths $\lambda\geqslant 2\pi/\epsilon$. Nevertheless, some of the bounds on q_1 are useful to us.

Many of the bounds on q_1 employ Cheeger's isoperimetric constant [36]. Isoperimetric inequalities relate the volume of a manifold to its surface area. Cheeger's constant is defined to be

$$h_C=\inf_S\frac{\mathrm{Vol}(S)}{\min\{\mathrm{Vol}(M_1),\mathrm{Vol}(M_2)\}}. \tag{5.7}$$

Here S runs through all compact codimension[f] one submanifolds which divide M into two disjoint submanifolds M_1, M_2 with common boundary $S=\partial M_1=\partial M_2$. A familiar example is the two-sphere. In this case M_1 and M_2 are both hemispheres, $S=\partial M_1$ is a great circle and we find $h_C(S^2)=1$.

Using his isoperimetric constant, Cheeger [36] derived the lower bound

$$q_1^2\geqslant\frac{h_C^2}{4}. \tag{5.8}$$

A decade later Buser [37] derived the upper bound

$$q_1^2\leqslant 4h_C+10h_C^2. \tag{5.9}$$

Cheeger's bound is valid for arbitrary closed manifolds in any dimension. Buser provided a general bound valid in any dimension for any closed manifold with bounded Ricci curvature. We have quoted Buser's bound in the form relevant for 3-manifolds with constant negative curvature. Given a 3-manifold Σ, we can in principle calculate Cheeger's constant and subsequently use it to place bounds on q_1. Recasting Cheeger's inequality in terms of wavelengths we find the maximum wavelength is bounded from above by

$$\lambda_{\max}\leqslant\frac{4\pi}{\sqrt{h_C^2-4}}. \tag{5.10}$$

Similarly, Buser's inequality provides a lower bound on the maximum wavelength:

$$\lambda_{\max}\geqslant\frac{2\pi}{\sqrt{10h_C^2+4h_C-1}}. \tag{5.11}$$

If $h_C>2$ we would learn that $\lambda_{\max}<\infty$. That is, there would be a long wavelength cut-off. Similarly, if $h_C>2\sqrt{1+4\pi^2}\approx 12.7$ we would learn that $\lambda_{\max}<1$ and therefore no modes with $\lambda>1$. On the other hand, an interesting lower bound occurs when $h_C<(\sqrt{14+40\pi^2}-2)/10\approx 1.82$. In this case the manifold supports perturbations beyond the curvature scale.

As we discuss below, the value of h_C is not known for most manifolds, but it can in principle be calculated numerically. There are however some special examples where h_C can be given a tight upper bound. Cheeger's constant is found by simultaneously minimizing $\mathrm{Vol}(S)$ while maximizing $\mathrm{Vol}(M_1)\leqslant\mathrm{Vol}(M_2)$. The two conditions can separately be satisfied by choosing S to be totally geodesic and taking $\mathrm{Vol}(M_1)=\mathrm{Vol}(M_2)=\mathrm{Vol}(M)/2$. One way to satisfy both of these conditions simultaneously is to find an involution on M that fixes S and interchanges M_1 and M_2. Then S is necessarily totally geodesic and M_1 and M_2 are mirror images of each other. This partition provides a local minimum for the ratio $\mathrm{Vol}(S)/\min(\mathrm{Vol}(M_1),\mathrm{Vol}(M_2))$, but it might not yield the global minimum required by the infinum in Eq. (5.7). Some interesting examples are known where S is a genus $g\geqslant 2$ surface and the ratio $\mathrm{Vol}(S)/\mathrm{Vol}(M)$ is maximized, i.e. these examples have the largest value of h_C for manifolds that separate along a totally geodesic boundary [38]. Written as a function of genus, the volume of S_g is $4\pi(g-1)$ and the volume of M is given by

$$\mathrm{Vol}(M_g)=g\left[-8\int_0^{\pi/4}\log|2\sin u|\,du-3\int_0^{\pi/3g}\operatorname{arccosh}\left(\frac{\cos v}{2\cos v-1}\right)dv\right]. \tag{5.12}$$

For these manifolds, the bounds on h_C range from $h_C\leqslant 1.9477$ for $g=2$ to $h_C\leqslant 3.43$ in the infinite genus limit. The genus 2 case is interesting since it tells us that there is a closed manifold with volume 12.904 that supports wavelengths $\lambda>0.94$. Furthermore, any other manifold that can be cut along a genus 2 surface will have larger volume and hence a lower isoperimetric constant h_C. These manifolds will in turn support even longer wavelength modes.

In principle it should be possible to provide a numerical estimate of Cheeger's constant for arbitrary manifolds by

trying a number of trial partitions. The best partitions could then be varied slightly and the search continued until the optimal partition is found. A judicious choice for the original trial partitions would ensure rapid convergence. The form of Cheeger's constant (5.7) suggests that the trial partitions should employ fairly smooth surfaces S that divide Σ into two approximately equal sized pieces. At present no numerical algorithm has been written, but it is hoped that the facility will be available in later releases of the SNAPPEA program [27].

In the absence of numerical results we have to resort to analytic estimates. An upper bound for Cheeger's constant can be derived using geodesic balls [39]:

$$h_C \leqslant \frac{\partial \ln V(\chi,\mathbf{x})}{\partial \chi}. \tag{5.13}$$

Here $V(\chi,\mathbf{x})$ is the volume of a geodesic ball with radius χ centered at $\mathbf{x}\in\Sigma$. The radius of the ball must be larger than the injectivity radius[c] $r_{\rm inj}$, but small enough so that $V(\chi,\mathbf{x})<\mathrm{Vol}(\Sigma)/2$. A lower bound for Cheeger's constant is quoted by Gallot [40]:

$$h_C \geqslant \frac{4\sqrt{\alpha}}{\mathrm{diam}(\Sigma)(\sinh\sqrt{\alpha}+\sqrt{\alpha})}, \tag{5.14}$$

where

$$\alpha \geqslant (\mathrm{diam}(\Sigma))^2 \quad \text{and} \quad \alpha \in \mathbf{Z}. \tag{5.15}$$

Notice that Eqs. (5.13) and (5.10) can be combined to show that manifolds with diameters smaller than 0.9195 have $q_1 \geqslant 1$ and thus no supercurvature modes. Applying the above bounds to Thurston's manifold [which has $r_{\rm inj}=0.289$, $0.868 \leqslant \mathrm{diam}(\Sigma_{\rm Th}) \leqslant 0.88$ and $\mathrm{Vol}(\Sigma_{\rm Th})=0.9814$] we find

$$2.09 \leqslant h_C(\Sigma_{\rm Th}) \leqslant 6.42, \tag{5.16}$$

and

$$1.04 \leqslant q_1 \leqslant 20.9. \tag{5.17}$$

Thus, Thurston's manifold does not support supercurvature modes (i.e. modes with complex wavelengths), but modes with wavelengths larger than the curvature scale are not ruled out.

Other bounds on q_j exist that do not use Cheeger's constant. Cheng [41] provides the bound

$$q_j^2 \leqslant 1+\frac{8(1+\pi^2)j^2}{\mathrm{diam}(\Sigma)^2}, \tag{5.18}$$

and Buser [42] provides the bound

$$q_j^2 \leqslant 1+c\left(\frac{j}{\mathrm{Vol}(\Sigma)}\right)^{2/3}, \quad c>1, \tag{5.19}$$

but the constant c is not quoted explicitly. Cheng derived his bound by first proving that the eigenvalues q_j in a closed manifold Σ are always lower than the first eigenvalue of an open geodesic ball with the same curvature and radius $\chi_0 = \mathrm{diam}(\Sigma)/(2j)$. The bound quoted in Eq. (5.18) is not very sharp since Cheng considered manifolds with arbitrary curvature. Here we derive a new, sharper bound by specializing to three-dimensional manifolds with constant negative curvature. The first eigenvalue of an open geodesic ball of radius χ_0 is found by solving the equation $(\Delta+q^2)Q=0$ with the boundary conditions

$$\frac{dQ}{d\chi}(0)=0, \quad Q(\chi_0)=0. \tag{5.20}$$

The eigenfunction with lowest eigenvalue is radial ($\ell=0$, $m=0$),

$$Q^{q00}(\chi)=\frac{\sin(\sqrt{q^2-1}\chi)}{\sqrt{q^2-1}\sinh\chi}, \tag{5.21}$$

and the boundary conditions demand that

$$q_1^2=1+\frac{\pi^2}{\chi_0^2}. \tag{5.22}$$

From this we derive the bound on the eigenvalues of Σ:

$$q_j^2 \leqslant 1+\left(\frac{2\pi j}{\mathrm{diam}(\Sigma)}\right)^2. \tag{5.23}$$

Translated into a bound on the allowed wavelengths this reads

$$\lambda_j \geqslant \frac{\mathrm{diam}(\Sigma)}{j}. \tag{5.24}$$

Thus, the maximum wavelength, λ_1, is at least as large as the diameter. The diameter is constrained to lie in the range

$$r_- < r_+ \leqslant \mathrm{diam}(\Sigma) \leqslant 2r_+. \tag{5.25}$$

Here r_- is the inradius[g] and r_+ is the outradius[e]. The geometrical constants for a selection of SNAPPEA's manifolds are collected in Table II. The volume and injectivity radius are both topological invariants while the in- and outradii depend on the choice of basepoint for the Dirichlet domain. The diameter can be found by forming the supremum

TABLE II. Scenes from the SNAPPEA census.

Σ	Vol	r_-	r_+	$r_{\rm inj}$
m003(−3,1)	0.9427	0.5192	0.7525	0.2923
m003(−2,3)	0.9814	0.5354	0.7485	0.2890
s556(−1,1)	1.0156	0.5276	0.7518	0.4157
m006(−1,2)	1.2637	0.5502	0.8373	0.2875
m188(−1,1)	1.2845	0.5335	0.9002	0.2402
v2030(1,1)	1.3956	0.5483	1.0361	0.1831
m015(4,1)	1.4124	0.5584	0.8941	0.3971
s718(1,1)	2.2726	0.6837	0.9692	0.1696
m120(−6,1)	3.1411	0.7269	1.2252	0.1570
s654(−3,1)	4.0855	0.7834	1.1918	0.1559
v2833(2,3)	5.0629	0.7967	1.3322	0.2430
v3509(4,3)	6.2392	0.9050	1.3013	0.1729

TABLE III. Diameters and eigenvalue bounds.

Σ	diam	q_1 min	q_1 max
m003(−3,1)	0.843	1.08	7.52
m003(−2,3)	0.868	1.04	7.31
s556(−1,1)	0.833	1.09	7.61
m006(−1,2)	1.017	0.82	6.26
m188(−1,1)	0.995	0.84	6.40
v2030(1,1)	1.082	0.77	5.90
m015(4,1)	0.923	0.98	6.88
s718(1,1)	1.439	0.53	4.48
m120(−6,1)	1.694	0.45	3.84
s654(−3,1)	1.946	0.36	3.38
v2833(2,3)	1.701	0.45	3.83
v3509(4,3)	1.802	0.39	3.63

$$\mathrm{diam}(\Sigma)=\sup_{\mathbf{0}}\{r_+\}, \tag{5.26}$$

where the supremum is taken over all choices of basepoint. Using a more direct numerical method we were able to compile a collection of sharp lower bounds for the diameter. Our method ensures that the true diameter is within ~0.01 of the lower bounds quoted in Table III. Also listed are upper and lower bounds on the first eigenvalue of the Laplacian derived using the inequalities quoted in this section.

It is interesting to note that the length of the shortest geodesic (twice the length of the injectivity radius[c] r_{inj}) does not grow with the volume. Even the largest manifolds in the SNAPPEA census, with volumes ~6, have geodesics as short as 0.3 in curvature units. This is consistent with Thurston's assertion [15] that the expectation value for the length of the shortest loop at an arbitrary point in a generic hyperbolic 3-manifold lies in the range $0.5\rightarrow 1$. This suggests that even relatively large manifolds still make for interesting small universe models.

Having established that generic compact hyperbolic 3-manifolds support modes with wavelengths exceeding the curvature scale, we have partially answered the question we set out to answer. Even neglecting the integrated Sachs-Wolfe effect, our results show that compact hyperbolic models are able to support the long wavelength modes required to produce large angle anisotropy on the surface of last scatter. A complete answer would require a knowledge of the spectral density at long wavelengths, as a few isolated subcurvature modes could not support significant large angle power on the SLS. In contrast, even a single supercurvature mode ($q_1<1$) could greatly enhance the large angle power [43]. Preliminary results from Bond *et al.* [25] using the method of images point to a reduced spectral density at long wavelengths. Unfortunately, their method is unable to detect supercurvature modes, so the most important part of the spectrum might be missing.

We can supplement the preceding discussion using a theorem due to Buser [44] which states that there exist finite volume compact hyperbolic 3-manifolds with an arbitrarily large number of modes with arbitrarily long wavelength. This theorem proves that any attempt to exclude *all* compact hyperbolic models on the basis of a lack of long wavelength power is doomed to failure. Admittedly, the manifolds considered by Buser have large diameters, but they also have small injectivity radii so they describe models that are multiconnected on scales smaller than the curvature scale. The fundamental cells for these manifolds are highly anisotropic, which may bring them into conflict with observations, but this is not certain since the face identifications tend to mix all three spatial directions and thus apparent isotropy can be restored.

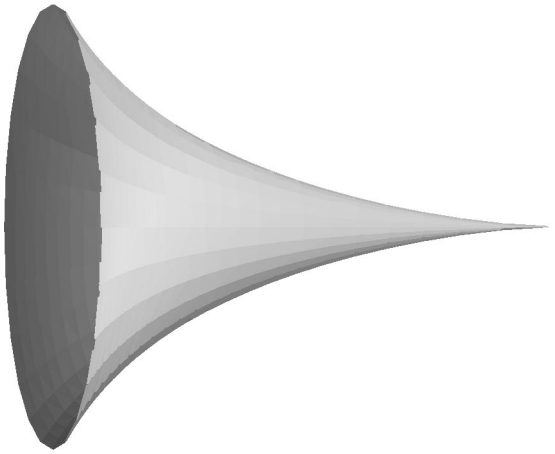

FIG. 4. A portion of the two-dimensional pseudosphere embedded in three-dimensional space.

VI. HORNED TOPOLOGIES

In this section we digress to consider a particular class of models that can be partially constrained by COBE data. In Ref. [10], Levin *et al.* describe the microwave sky in a universe with the topology of a hyperbolic toroidal horn. The topology they consider is the three-dimensional analogue of the two-dimensional pseudosphere. The pseudosphere, referred to as a cusp by mathematicians, is topologically equivalent to $S^1\times[0,\infty)$, where S^1 is a circle. Figure 4 shows a portion of the pseudosphere embedded in three-dimensional space. The pseudosphere is described in the upper half plane representation of H^2 by

$$d\sigma^2=\frac{dx^2+dz^2}{z^2}, \tag{6.1}$$

with the identifications $x=x+nL_x$ with $n\in\mathbf{Z}$. Cusps in d dimensions are analogously defined to be of the form $E^{d-1}\times[0,\infty)$ where E^{d-1} is a flat topology in $(d-1)$ dimensions. It should be emphasized that the line $z=\mathrm{const}$ connecting x and $x+L$ is not a geodesic. Geodesics in the upper half plane model appear as half-circles of the form $x^2+z^2=a^2$, perpendicular to the boundary plane.

The hyperbolic horn studied in Ref. [10] is of the form $T^2\times[0,\infty)$ where T^2 is the two-torus. In the upper half plane model of H^3,

$$d\sigma^2=\frac{dx^2+dy^2+dz^2}{z^2}, \tag{6.2}$$

the horn is defined by making the identifications $x=x+nL_x$ and $y=y+mL_y$. Since translations commute, the

horn's fundamental group is Abelian and geodesics on the horn are non-chaotic. This means that the horn's eigenmodes can be written down explicitly.

The calculational simplicity of the horn model is offset by some unappealing physical characteristics. Not only is the horn noncompact and infinite in volume, but it also suffers from severe global anisotropy. The anisotropy can be seen by moving to spherical coordinates centered at $(x,y,z)=(0,0,1)$. Our ghost images then appear at the points

$$\chi=\operatorname{arcsinh}\left[\operatorname{arccosh}\left(1+\frac{1}{2}(n^2L_x^2+m^2L_y^2)\right)\right],$$

$$\theta=\pm\arccos\left(\left[1+\frac{4}{(n^2L_x^2+m^2L_y^2)}\right]^{-1/2}\right),$$

$$\phi=\arcsin\left(\frac{mL_y}{\sqrt{n^2L_x^2+m^2L_y^2}}\right). \tag{6.3}$$

The ghost images are evenly distributed in the ϕ direction, but distant images pile up along the axis of the horn ($\theta=\pi/2$).

Because the horn's fundamental group is Abelian, there will be a long wavelength cut-off in directions orthogonal to the axis of the horn. In this respect the hyperbolic horn is similar to the flat topology $\Sigma=R\times T^2$. The difference is that the torus cross sections of the horn do not have fixed area. As we move away from the origin, the torus area decreases like

$$A(T^2)=\frac{1}{2}L_xL_y\exp(-2\sinh\chi). \tag{6.4}$$

This means that the wavelength cut-off gets shorter and shorter as we move toward the cusp. Moreover, the decrease is *doubly exponential* with increasing proper distance. This has the effect of suppressing all temperature fluctuations in the direction of the horn, leading to a ''flat-spot'' [10] in the microwave sky.

Considering that there are an infinite number of hyperbolic 3-manifolds to choose from, it might seem strange to focus on one particular example. However, it turns out that many manifolds have horn-like regions. To see why one needs to understand something about how hyperbolic 3-manifolds are constructed. According to Jørgensen's theorem [45], all finite volume hyperbolic 3-manifolds can be obtained by Dehn surgery on a finite number of link complements in S^3. A link complement is constructed by drilling out a solid tubular knot or link from spherical space. The complement of this link (i.e. the space outside the link) will almost always be topologically equivalent to a hyperbolic 3-manifold with one or more cusps. If one happened to live deep inside a cusp, the universe would look exactly like a toroidal horn.

While the finite volume of the cusped manifolds makes them more appealing than the basic hyperbolic horn, they are still non-compact. In order to arrive at compact models we need to perform Dehn surgery on the link. The surgery involves cutting out a portion of the link and replacing it with a solid torus that is first twisted around the link in some non-trivial way. Without going into details,[8] it is sufficient to note that the twisting can be parametrized by two integers (p,q). In the limit $p,q\to\infty$ with p,q relatively prime, the original cusped manifold is recovered. For small p,q the cusp can be completely removed. For large values of p,q the end of the cusp is rounded off leaving a ''horned manifold.'' If one happened to live deep inside one of the horns, the universe would look similar to how it does in the infinite toroidal horn. The exact correspondence is broken since Dehn surgery makes the fundamental group non-Abelian. This means that the geodesics will be chaotic and the eigenmodes complicated. Nonetheless, for high order Dehn fillings the chaos should be mild and it seems reasonable to expect a flat spot in the CMB if one lived in a horned region of the manifold.

The preceding considerations have shown that the results of Ref. [10] apply in certain regions of a large class of three manifolds. If we happened to live in one of these horned regions, we would see a severe suppression of CMB fluctuations along the horn. Levin *et al.* found that this effect was not masked by the integrated Sachs-Wolfe effect, so the COBE satellite would have detected flat spots in the CMB. However, the absence of flat spots is not a very strong constraint on us living in a cusped manifold. This is because cusps only account for a very small portion of a cusped manifold's volume. Therefore, it is very unlikely that we would be living in or near a cusp. If we make what topologists refer to as a ''thick-thin'' decomposition [46], we find that most of a manifold's volume is in the ''thick'' part and very little is in ''thin'' regions such as cusps. The chance that we live deep inside a cusp is even smaller since the volume of a cusp decreases as $\exp(-2e^{\chi})$, where χ is the proper distance down the cusp. We are far more likely to live in a thick portion of a manifold where the breaking of global isotropy is much less noticeable. The analysis of Levin *et al.* is not valid for observers that live in the thick portion of a manifold. The fundamental group of a cusped manifold is non-Abelian, but contains a normal Abelian subgroup of finite index, corresponding to isometries of the cusp. Inside a cusp the fundamental group is dominantly Abelian and the horn analysis holds, but in the thick part of the manifold the isometries are dominantly non-Abelian and the horn analysis does not hold. It would be interesting to extend the horn analysis to cusped manifolds with finite volume and to closed manifolds with horn-like regions.

In summary, it would be surprising if we did live in a horned region, and the results of Levin *et al.* confirm that we do not.

VII. POWER SPECTRA, WAVE NUMBERS AND MULTIPOLES

A. Generating the primordial power spectrum

The temperature fluctuations measured by COBE-DMR are thought to arise from the amplification of quantum fluctuations during an inflationary phase, or alternatively, from a network of topological defects. We will not consider the lat-

[8]See Thurston's book [46] or the appendix of Carlip's article [47] for a description of how to perform Dehn surgery.

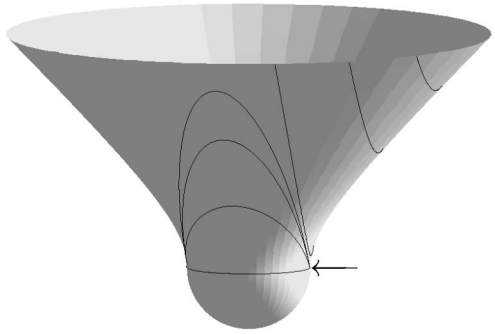

FIG. 5. The tunnelling configuration. The lines indicate constant time hypersurfaces. The arrow indicates the point on the S^3 Cauchy surface where the bubble nucleates. The region to the upper right of this point is the interior of the bubble, the region to the upper left remains in the false vacuum.

ter possibility as there appears to be a topological obstruction to the formation of topological defects in a small universe [48]. In the inflationary context, some fine tuning is required to avoid blowing the curvature scale outside the surface of last scatter. There are currently two scenarios for arriving at a negatively curved universe from inflation. The first is one-bubble inflation [49], the second is compact inflation [3]. Detailed calculations of the power spectrum have been performed for the one-bubble model, while little is known about the spectrum for compact inflation. Here we discuss how the one-bubble scenario relates to multiconnected models, and offer some speculations about the form of density perturbations produced by compact inflation.

1. One-bubble inflation

Since there is an explicit and well understood quantum tunnelling process underlying the one-bubble inflation scenario, it is possible to make definite predictions about the form of the primordial power spectrum [49]. The universe begins in an inflationary epoch driven by an inflaton field in a false vacuum state. During this epoch, any inhomogeneities are inflated away. Subsequently, a single bubble is nucleated, inside of which the inflaton field rolls toward its true minimum. Taking the inflaton to be described by a single real scalar field ϕ (several variants of this basic picture have been considered), surfaces of constant ϕ inside the bubble have constant negative curvature. Mathematically this process is described by an $O(4)$ symmetric Euclidean instanton—Euclidean de Sitter space with one special point. The bubble nucleation selects a preferred point in de Sitter space, breaking the full $O(5)$ symmetry down to $O(4)$. As shown in Fig. 5, the Euclidean instanton is matched onto its Lorentzian counterpart across a totally geodesic spatial hypersurface, $S^3=\partial S^4$. The matching surface is a Cauchy surface for the subsequent Lorentzian evolution. Owing to the $O(4)$ symmetry of the instanton, the bubble interior has the $SO(3,1)$ symmetry of hyperbolic space.

The question we need to ask is: can the one-bubble scenario be generalized to produce a hyperbolic universe with non-trivial spatial topology? The answer is no, unless one is willing to live with closed timelike curves. The only way non-trivial topology can enter into the picture is through the spatial topology of S^3, since the Lorentzian evolution is fully determined by specifying Cauchy data for the metric and matter fields on the initial S^3 Cauchy surface. Put differently, the solution is specified globally on the S^3 hypersurface but only locally in the direction normal to this surface. Let us start by considering the simplest non-trivial topology for the matching surface – the real projective space $RP^3\cong S^3/Z_2$. Taking the geometry shown in Fig. 5 as the universal cover, we find there is a clone of the bubble on the opposite side of de Sitter space. Since antipodal points in de Sitter space lie outside each other's light cone, the bubble and its clone never intersect. Inside the bubbles we have two copies of the same simply connected hyperbolic universe. While this sounds reasonable, we encounter a problem when trying to define quantum fields in this background as the instanton has topology RP^4 and is thus non-orientable. It is impossible to separate modes into positive and negative frequency components in such spacetimes. As we move on to consider more complicated topologies the situation gets worse. Once the number of clones exceeds two, the bubbles start to collide (self-intersect). Moreover, according to an observer inside the bubble, the spatial identifications on the spherical slicings become spatio-temporal identifications in hyperbolic space. These universes have closed time loops and there is no known prescription for defining a sensible quantum theory in such spacetimes.

So while the most complete calculations of the primordial power spectrum have been done in the context of one-bubble inflation, they cannot be generalized to models with compact hyperbolic sections. Indeed, if we do find evidence for non-trivial (purely) spatial topology, we would know that the one-bubble model is ruled out.

2. Compact inflation

In the compact inflation scenario the universe is taken to have compact hyperbolic spatial sections. The chaotic mixing that occurs in compact hyperbolic space is understood to have erased any initial density perturbations before vacuum domination is reached [3]. This prepares the ground for a necessarily short burst of inflation. It is the chaotic mixing that solves the horizon problem, and not the short period of inflation.

In order to calculate the quantum fluctuations in compact inflation we need to know the eigenmodes and the initial vacuum state, i.e. how the modes are populated. Once these are known we can evolve the quantum fluctuations to find the density perturbations at the end of inflation. At present we know neither the eigenmodes nor the correct vacuum state to choose. The situation is only slightly better for non-compact open inflation models, for while the eigenmodes are known, the choice of initial vacuum is not. Here we are referring to models other than the one-bubble model (see e.g. Ref. [11]). Another difficulty with open inflation stems from the short period of inflation being insufficient to solve the horizon problem. This problem is greatly exacerbated by the open universe Grishchuk-Zel'dovich effect [50], which demands that the pre-inflationary universe be smooth on scales one thousand times larger than the curvature scale. In a compact hyperbolic universe this is not a problem since the entire universe is typically no larger than the curvature scale. In a small universe there can be no ''monsters'' lurking over the horizon, for we already see all there is to see.

The generation of curvature perturbations in an open universe closely parallels that in a flat universe: Starting in some initial state, the perturbations evolve until they cross outside the Hubble horizon, whence they are frozen in. After inflation, the Hubble horizon expands to encompass perturbations of increasing wavelength. Once back inside the Hubble radius the perturbations can undergo further evolution. In an open universe the large scale perturbations are amplified by the ISW effect. Fluctuations with wavelengths much smaller than the curvature scale are insensitive to the curvature and evolve just as they do in the flat models. For these modes it seems reasonable to use the usual conformal vacuum initial conditions [11]. We anticipate the same should be true in compact hyperbolic models for fluctuations frozen in long after the topology scale exited the Hubble horizon. The situation is far more complicated near the curvature scale, as it is here that the geometry and topology of the background manifold become most important. On large angular scales there will be a delicate interplay between 6 main effects: (1) Amplification by the ISW effect; (2) Suppression by gravitational focusing; (3) Curvature distortions of the conformal vacuum; (4) Inflationary transients; (5) Finite size distortions of the conformal vacuum; (6) Reduced spectral density at long wavelengths. The first four of these effects are present in all open inflation models while the last two are unique to compact inflation. Taking into account effects (1) and (2) while neglecting effects (3) and (4) leads to an angular power spectrum with positive slope [51]. Of the remaining effects, it is likely that inflationary transients will boost the power on large scales while any reduction in the spectral density will tend to reduce power on large angular scales. The hardest questions to answer concern distortions to the conformal vacuum, as these can only be answered in the context of quantum cosmology by repeating the sort of calculations performed by Halliwell and Hawking for closed models [52]. Until this is done, and until more is known about the eigenmode spectra, no firm predictions can be made about the power spectrum on large angular scales.

B. Wave numbers and multipoles

In Sec. II we described how the ISW effect alters the flat space relationship between wave number k and multipole number ℓ. In flat space, the dominant contribution to the $\ell^{\rm th}$ multipole comes from fluctuations with wave number $k_{sls} \sim \ell+1$. This simple relationship between k and ℓ translates into a simple relationship between the power spectrum of density perturbations, $P(k)=|\delta_k|^2$, and the r.m.s. temperature fluctuations in each multipole, $P(l)=(\ell(\ell+1)C_\ell)^{1/2}$, where $C_\ell=\langle|a_{\ell m}|^2\rangle$. The standard example is a flat universe with power-law spectrum $P(k)\propto k^n$, where it is found that

$$C_\ell \propto \frac{\Gamma[3-n]}{\Gamma[(4-n)/2]^2}\frac{\Gamma[(2\ell+n-1)/2]}{\Gamma[(2\ell+5-n)/2]}. \qquad (7.1)$$

Already we have seen that the ISW effect breaks this correspondence on large angular scales in an open universe. In compact hyperbolic space there is an additional effect that tends to spread power from different scales into each multipole. Physically, this effect is related to quantum chaos and the mixing properties of compact hyperbolic spaces. Mathematically, the effect arises because a multipole expansion attempts to use a basis of smooth analytic functions to represent the non-analytic wavefunctions. According to Berry [53], if $\Psi_k(\mathbf{x})$ is an eigenmode of H^3/Γ, then the coefficients $a_{\ell m}$ in the expansion

$$\Psi_k(\mathbf{x})=\sum_\ell \sum_{m=-\ell}^{m=\ell} \delta_k a_{\ell m} X_k^\ell(\chi) Y_m^\ell(\theta,\phi), \qquad (7.2)$$

are essentially random variables with amplitude virtually independent of ℓ. At small wave numbers and large angular scales, there is almost no correlation between k and ℓ in compact hyperbolic space. The convergence of the sum (7.2) is inherently slow since it comes not from a decrease in the expansion coefficients, but from the decay of $X_k^\ell(\chi)$ across the fundamental domain.

Some concrete results are known in two dimensions that nicely illustrate this effect. Consider a genus 2 (hyperbolic) surface with eigenmodes $\Psi_k(\mathbf{x})$. The analogue of Eq. (7.2) is then

$$\Psi_k(\mathbf{x})=\sum_{m=-\infty}^{m=\infty} \delta_k a_m Y_k^m(\chi) e^{im\phi}. \qquad (7.3)$$

Here it is known that

$$c_1|m|^{-1/2} \leqslant |a_m| < c_2|m|^{1/2}, \qquad (7.4)$$

where c_1 and c_2 are constants. It is thought that the lower bound $|a_m|\sim|m|^{-1/2}$ is a good estimate of the true behavior [31]. This leads to an essentially flat angular power spectrum[9] $P(m)=(2|m|)^{1/2}|a_m|=$const, regardless of the perturbation spectrum δ_k.

The above results suggest a novel way of arriving at a nearly flat Harrison-Zeldovich spectrum, regardless of the underlying physical process that produces the fluctuations. We expect that this redistribution of power will be most efficient on large angular scales and least efficient on small angular scales. Our reasoning is that long wavelength modes are the hardest to approximate by analytic functions since they are most affected by the complicated periodic boundary conditions imposed by the topology. Conversely, the short wavelength modes are less sensitive to global effects, and therefore well approximated by the corresponding eigenmodes of infinite hyperbolic space.

VIII. CONCLUSIONS

A hyperbolic drum produces a rich and complex sound. A compact hyperbolic universe is likewise infinitely more complex than its spherical or Euclidean counterparts. The simple methods used to constrain flat models do not work when space is negatively curved. The eigenmodes in a compact hyperbolic space can only be calculated using sophisticated methods developed to treat quantum chaos. Moreover, hyperbolic models do not suffer the simple long wavelength cut-off used to exclude toroidal models.

In addition to the issue of what fluctuations are supported

[9] $P(m)$ is the two-dimensional analogue of the usual angular power spectrum, $P(\ell)$, in three-dimensions.

on the last scattering surface, there is also the issue of what exactly it was that COBE measured. In a compact hyperbolic universe the curvature radius provides a natural length scale, $R_0 = H_0^{-1}/\sqrt{1-\Omega_0}$. The curvature radius sets the length scale where we might hope to find the first evidence that we live in a multiply connected universe. The curvature radius also sets the angular scale beyond which fluctuations in the cosmic microwave background radiation no longer originate from the last scattering surface. This confluence of physical scales is very unfortunate for COBE since it means that the ISW effect takes over just when things get interesting. Fortunately the next generation of CMB satellites will be able to probe much smaller angular scales, so the ISW effect will not obscure their view of the large scale topology of the universe.

The search for multi-connectedness in our universe is not over. It has barely begun.

ACKNOWLEDGMENTS

We are indebted to Jeff Weeks for his extensive expert advice on topology and the workings of SNAPPEA. Our knowledge of cusped manifolds was greatly enhanced by discussions with Bill Thurston and Jeff Weeks. We thank the topologists Bob Brooks, Pat Callahan, Ruth Kellerhals and Alan Reid for sharing their knowledge on the eigenvalue spectra. We have also enjoyed informative discussions with Dick Bond, Andrew Chamblin, Fay Dowker, Gary Gibbons and Janna Levin. N. Cornish was supported by PPARC grant GR/L21488. D. Spergel was supported by the NASA grant for the Microwave Anisotropy Probe. G. Starkman was supported by a NSF career grant.

APPENDIX

The following glossary of terms describes the basic mathematical quantities used in our discussion of topology. Our definitions are designed to be more pictorial than the usual formal definitions found in the mathematical literature.

[a] Betti numbers. The zeroth Betti number, b_0, counts the number of disconnected regions in a manifold. The first Betti number, b_1, counts the number of incontractible loops. The second Betti number, b_2, counts the number of incontractible surfaces. Higher Betti numbers are similarly defined. The first Betti number is equal to the rank of the free Abelian part of the first homology group $H_1(\Sigma)$. In other words, the first Betti number is equal to the number of generators of $H_1(\Sigma)$ that are not subject to any relations save those that make the group Abelian. Poincare duality relates the various Betti numbers so that in d-dimensions $b_i = b_{(d-i)}$.

[b] Injectivity radius function. The injectivity radius of a point $p \in M$, $r_{\rm inj}(p)$, is the radius of the largest coordinate chart that can be centered at p. Since a coordinate chart breaks down when any geodesic refocuses, the injectivity radius of a point is half the length of the shortest geodesic connecting p to itself.

[c] Injectivity radius. The injectivity radius of a manifold, $r_{\rm inj}(M)$, is the smallest injectivity radius of any point in the manifold, i.e.

$$r_{\rm inj}(M) = \inf_p r_{\rm inj}(p \in M). \tag{A1}$$

Thus, $r_{\rm inj}(M) = l_{\rm min}/2$, where $l_{\rm min}$ is the length of the shortest geodesic in (M,g).

[d] Diameter. The diameter, diam(M), of a manifold (M,g) is the greatest distance between any two points on the manifold.

[e] Outradius. The outradius, r_+, of a compact hyperbolic manifold fixes the size of the smallest hyperbolic ball that can be used to enclose the fundamental cell.

[f] Codimension. The codimension is a complementary dimension. A n-dimensional hypersurface living in a d-dimensional space has codimension $d-n$.

[g] Inradius. The inradius, r_-, is the radius of the largest simply connected geodesic ball in (M,g). In other words, r_- is the largest distance any point in the manifold can be from its closest image. For a compact hyperbolic manifold, the inradius fixes the size of the largest hyperbolic ball that can be placed inside the fundamental cell.

[1] M. Kac, Am. Math. Monthly **73**, 1 (1966).
[2] For a review see M. Lachieze-Rey and J-P. Luminet, Phys. Rep. **254**, 135 (1995).
[3] N.J. Cornish, D. Spergel and G. Starkman, Phys. Rev. Lett. **77**, 215 (1996).
[4] N.J. Cornish, D. Spergel and G. Starkman, ''Circles in the Sky: Finding Topology with the Microwave Background Radiation,'' gr-qc/9602039.
[5] C. L. Bennett *et al.*, Astrophys. J. **464**, L1 (1996).
[6] I.Y. Sokolov, JETP Lett. **57**, 617 (1993).
[7] A.A. Starobinsky, JETP Lett. **57**, 622 (1993).
[8] D. Stevens, D. Scott, and J. Silk, Phys. Rev. Lett. **71**, 20 (1993).
[9] A. de Oliveira Costa and G.F. Smoot, Astrophys. J. **448**, 477 (1995); A. de Oliveira Costa, G.F. Smoot, and A.A. Starobinsky, *ibid.* **468**, 457 (1996).
[10] J.J. Levin, J.D. Barrow, E.F. Bunn, and J. Silk, Phys. Rev. Lett. **79**, 974 (1997).
[11] D. H. Lyth and E. D. Stewart, Phys. Lett. B **252**, 336 (1990).
[12] N. Gouda, N. Sugiya, and M. Sasaki, Prog. Theor. Phys. **85**, 1023 (1991).
[13] M. Kamionkowski and D. Spergel, Astrophys. J. **432**, 7 (1994).
[14] J.R. Gott III, Mon. Not. R. Astron. Soc. **193**, 153 (1980); R. Lehoucq, M. Lachieze-Rey, and J.P. Luminet, Astron. Astrophys. **313**, 339 (1996); B. F. Roukema and A. C. Edge, Mon. Not. R. Astron. Soc. **292**, 105 (1997).
[15] W. P. Thurston (private communication).
[16] V. F. Mukhanov, R. H. Brandenberger, and H. A. Feldman, Phys. Rep. **215**, 203 (1992).
[17] M. Zaldarriaga and D. Harari, Phys. Rev. D **52**, 3276 (1995).

[18] D.N. Spergel and M. Zaldarriaga, Phys. Rev. Lett. **79**, 2180 (1997).
[19] M.C. Gutzwiller, J. Math. Phys. **11**, 1791 (1970); **12**, 343 (1971).
[20] M.V. Berry and J.P. Keating, J. Phys. A **23**, 4839 (1990).
[21] O. Agam and S. Fishman, J. Phys. A **26**, 2113 (1993).
[22] L. Abbot and R. Shaefer, Astrophys. J. **308**, 462 (1986).
[23] J. Ratcliffe, *Foundations of Hyperbolic Manifolds*, Graduate texts in Math. **149**, (Springer-Verlag, Berlin, 1994).
[24] J.R. Bond, D. Pogosyan and T. Souradeep, astro-ph/9702212, 1997.
[25] T. Souradeep, talk given at the Cleveland Topology and Cosmology meeting, 1997.
[26] J. Milnor, J. Diff. Geom. **2**, 1 (1968).
[27] J. Weeks, SNAPPEA: A computer program for creating and studying hyperbolic 3-manifolds, available at http://www.geom.umn.edu:80/software
[28] W.P. Thurston, Bull. Am. Math. Soc. **6**, 357 (1982).
[29] M. Nakahara, *Geometry, Topology and Physics* (Hilger, Bristol, 1990), pg. 113.
[30] H.P. McKean, Commun. Pure Appl. Math. **25**, 225 (1972).
[31] N.L. Balazs and A. Voros, Phys. Rep. **143**, 109 (1986).
[32] S.V. Matveev and A.T. Fromenko, Russian Math. Surveys **43:1** 3 (1988).
[33] J. Wolf, *Spaces of Constant Curvature* (Publish or Perish, Wilmington, 1984).
[34] G.D. Mostow, *Ann. Math. Studies* (Princeton University Press, Princeton, NJ, 1973), Vol. 78; G. Prasad, Invent. Math. **21**, 255 (1973).
[35] D. Gabai, G. R. Meyerhoff, and N. Thurston, MSRI Report No. 1996-058, 1996.
[36] J. Cheeger, in *Problems in Analysis*, A symposium in honour of S. Bochner (Princeton University Press, Princeton, NJ, 1970).
[37] P. Buser, Ann. Sci. Ec. Norm. Sup. **15**, 213 (1982).
[38] Y. Miyamoto, Topology **33**, 613 (1994).
[39] R. Brooks, in *Topology '90*, edited by B. Apanasov, W.D. Neumann, A.W. Reid, and L. Siebenmann (Ohio State University Mathematical Research Institute Publications, Columbus, OH, 1992), Vol. 1, p. 61.
[40] S. Gallot, C. R. Seances Acad. Sci., Ser. 1 **296**, 333 (1983).
[41] S.-Y. Cheng, Math. Z. **143**, 289 (1975).
[42] P. Buser, Math. Z. **165**, 107 (1977).
[43] J. Garcia-Bellido, Phys. Rev. D **54**, 2473 (1996).
[44] P. Buser, in *Geometry of the Laplace Operator*, Proceedings of the Symposium in Pure Mathematics of the American Mathematical Society, Honolulu, Hawaii, 1979, edited by R. Osserman and A. Weinstein, Proc. Symp. Pure Math. **XXXVI** (American Mathematical Society, Providence, RI, 1980), p. 29.
[45] W. P. Thurston, The Geometry and Topology of Three Manifolds, Lecture Notes, 1979.
[46] W. P. Thurston, *Three-Dimensional Geometry and Topology*, edited S. Levy (Princeton University Press, Princeton, NJ, 1997).
[47] S. Carlip, Phys. Rev. D **46**, 4387 (1992).
[48] J.-P. Uzan and P. Peter, Phys. Lett. B **406**, 20 (1997).
[49] J.R. Gott, Nature (London) **295**, 304 (1982); M. Bucher, A.S. Goldhaber and N. Turok, Phys. Rev. D **52**, 3314 (1995).
[50] J. Garcia-Bellido, A. R. Liddle, D. H. Lyth, and D. Wands, Phys. Rev. D **52**, 6750 (1995).
[51] N. Sugiyama and J. Silk, Phys. Rev. Lett. **73**, 509 (1994).
[52] J.J. Halliwell and S.W. Hawking, Phys. Rev. D **31**, 1777 (1985).
[53] M.V. Berry, J. Phys. A **10**, 2083 (1977); M.V. Berry, N. L. Balazs, M. Tabor, and A. Voros, Ann. Phys. (N.Y.) **122**, 26 (1979).